Empirical test of the Kelvin relation in thermoelectric nanostructures

Cite as: Appl. Phys. Lett. 124, 113505 (2024); doi: 10.1063/5.0197974 Submitted: 15 January 2024 · Accepted: 4 March 2024 · Published Online: 14 March 2024













AFFILIATIONS

Department of Physics, The University of Texas at Dallas, Richardson, Texas 75080, USA

ABSTRACT

Thermoelectric (TE) nanostructures with dimensions of ~100 nm can show substantially better TE properties compared to the same material in the bulk form due to charge and heat transport effects specific to the nanometer scale. However, TE physics in nanostructures is still described using the Kelvin relation (KR) $\Pi = \alpha T$, where Π is the Peltier coefficient, α the thermopower, and T the absolute temperature, even though derivation of the KR uses a local equilibrium assumption (LEA) applicable to macroscopic systems. It is unclear whether nanostructures with nanostructures with dimensions on the order of an inelastic mean free path satisfy a LEA under any nonzero temperature gradient. Here, we present an experimental test of the KR on a TE system consisting of doped silicon-based nanostructures with dimensions comparable to the phonon-phonon and electron-phonon mean-free-paths. Such nanostructures are small enough that true local thermodynamic equilibrium may not exist when a thermal gradient is applied. The KR is tested by measuring the ratio Π/α under various applied temperature differences and comparing it to the average T. Results show relative deviations from the KR of $|(\Pi/\alpha)/T - 1| \le 2.2\%$, within measurement uncertainty. This suggests that a complete local equilibrium among all degrees of freedom may be unnecessary for the KR to be valid but could be replaced by a weaker condition of local equilibrium among only charge carriers.

Published under an exclusive license by AIP Publishing. https://doi.org/10.1063/5.0197974

Integration of thermoelectric (TE) materials with microelectronics is a possible means to make Internet-of-Things devices energy autonomous or to locally cool hotspots in high-performance integrated circuits. In the effort to scale down the size of TE devices to be compatible with microelectronic applications, it was found that nanostructures with dimensions of order 100 nm could have superior TE properties compared to the same material in the bulk form. Much higher TE figures-of-merit ZT^{2-4} as well as enhanced TE power factors $\alpha^2 \sigma$ (Refs. 5–8) have been reported in nanostructured TE materials. Here, α is the thermopower, σ is the electrical conductivity, κ is the sum of lattice and charge thermal conductivities, T is the average temperature of a thermopile, and $Z = \alpha^2 \sigma / \kappa$. These reports attributed improvements in TE properties to scattering and interface effects important to charge and heat transport in nanostructures but not in the bulk form.

Such findings provide evidence that TE physics may differ significantly in nanostructures vs bulk materials, but analysis of TE performance in nanostructured thermopiles still assumes applicability of the Kelvin relation (KR) $\Pi = \alpha T$, where Π is the Peltier coefficient. While the KR is a bedrock of macroscopic TE physics, its validity when

applied to nanostructures is open to question as explained by the following argument. The KR is a specific type of Onsager reciprocal relation (ORR)^{10,11} applied to TE phenomena.¹² The ORR was developed to describe irreversible thermodynamic processes in macroscopic systems, and its derivation relies on a local equilibrium assumption (LEA). The LEA simplifies a macroscopic nonequilibrium system by regarding it as composed of an ensemble of subsystems each in its own local equilibrium. Modern theoretical explorations of the ORR¹⁴⁻¹⁸ argue that the ORR is valid if the LEA can be considered a good assumption. However, the LEA is questionable for nanostructures because, as emphasized by several authors, 19-22 the characteristic length scale of a subsystem should be an inelastic mean-free-path, because several energy exchanges must occur among all degrees-offreedom for a subsystem to thermalize to local equilibrium. Nanostructures with dimensions of order an inelastic mean-free-path have too few energy exchanging collisions to equilibrate under a thermal perturbation. In crystalline solids, heat is carried by both charges and phonons, so a true local equilibrium must involve equilibration among all charge and lattice degrees-of-freedom. This sets the relevant length scale as the longest of the various inelastic mean-free-paths.

²Texas Instruments Incorporated, Dallas, Texas 75243, USA

a) Author to whom correspondence should be addressed: marklee@utdallas.edu

In most crystalline semiconductors near 300 K, the electron–phonon and phonon–phonon inelastic mean-free-paths ℓ are \geq 100 nm, so the LEA may not be a good assumption for most semiconductor nanostructures.

In this paper, we report an experimental test of the KR in doped $Si_{0.97}Ge_{0.03}$ nanostructures having nominal dimensions 80×350 \times 750 nm³. The KR was tested following the method described in Ref. 23, where the relation $\Pi/\alpha = T$ was empirically validated in bulk Bi₂Te₃ thermopiles to ≤0.5% measurement uncertainty.²³ For the Si_{0.97}Ge_{0.03} nanostructures at the dopant concentrations used, the inelastic phonon-phonon and electron-phonon mean-free-paths in Si are estimated to be $\ell \sim 100-300$ nm near 300 K. ^{24,25} While the effect of 3% Ge substitution on ℓ has not been investigated, as long as these inelastic lengths are not very strongly affected, these nanostructures are of order ℓ in dimension. Taking $\ell = 300 \, \mathrm{nm}$ as the longest of these mean-free-paths, the nanostructure volume is $0.8\ell^3$, so on average there would be ≤1 energy-exchanging collision between charge carrier and phonon, or phonon and phonon, moving through the nanostructure volume. As a consequence, under a temperature gradient $\nabla T \neq 0$, complete local equilibrium may not be achieved between charges and lattice. Nonetheless, we empirically find that the KR result remains correct to within 2% measurement uncertainty, i.e., $|(\Pi/\alpha)/T - 1| < 0.02$.

The TE devices used in this experiment consisted of arrays of $\mathrm{Si}_{0.97}\mathrm{Ge}_{0.03}$ "nanoblades" with the previously stated dimensions fabricated on a Si wafer using an industrial "65-nm technology node" moat etch process as described in detail previously. $^{26,27}\mathrm{Si}_{0.97}\mathrm{Ge}_{0.03}$ was used because it has larger ZT and hence gives better signal-to-noise in TE measurements compared to pure Si. Figure 1 shows (a) an illustration and (b) a cross-sectional scanning electron microscope image of a thermopile formed by arrays of doped nanoblades. The n-type nanoblades were doped at $n=4.3\times10^{17}\,\mathrm{cm}^{-3}$, and the p-type nanoblades were doped at $p=2.2\times10^{17}\,\mathrm{cm}^{-3}$, as determined by technology computeraided design process modeling. Five separate thermopiles of identical design were measured to monitor reproducibility.

A temperature difference was applied between the top and bottom of a thermopile (along its 350 nm height dimension). A resistive

thermistor integrated in-chip above the thermopile provided a heat source, and the metal chuck of the probe station holding the test chip acted as a heat sink [see Fig. 1(a)]. Thermistor temperature, $T_{\rm source}$ was determined by measuring the thermistor's resistance $R_{\rm therm} = V_{\rm therm}/I_{\rm therm}$, where $V_{\rm therm}$ was the voltage bias applied, and $I_{\rm therm}$ the measured current through the thermistor. The thermistor's temperature coefficient-of-resistance and its equilibrium resistance at ambient temperature (296 K) were calibrated using the procedure described in Ref. 26. Heat sink temperature, $T_{\rm sink}$, was measured using a commercial calibrated diode thermometer embedded in the chuck. $T_{\rm sink}$ could be elevated using a resistive heater in the chuck.

The applied temperature difference $\Delta T = (T_{\rm source} - T_{\rm sink})$ was thus controlled but was not the actual temperature difference $\Delta T'$ across the nanoblade thermopile, indicated in Fig. 1(a), due to parasitic series thermal resistances. Existence of nonzero $\Delta T'$ across both ends of the thermopile was confirmed by observation of open circuit voltage $(V_{\rm OC})$ and short circuit current $(I_{\rm SC})$ both linearly dependent on ΔT , see Figs. 2(a) and 2(b). While $\Delta T'$ was not directly measured, $(\Delta T'/\Delta T)$ can be determined with good accuracy either by constructing a detailed thermal circuit model, as in Ref. 26, or by noting that the ratio of the measured thermopower, $\alpha_{\rm meas}$, to true thermopower value 28 from literature, α , is $(\alpha_{\rm meas}/\alpha) = (\Delta T'/\Delta T)$. Both methods gave $(\Delta T'/\Delta T) = 0.20 \pm 0.02$. Temperatures $T_{\rm source}$ and $T_{\rm sink}$ were set so that ΔT could be varied from 20 to 110 K, making $\Delta T' \approx 4$ to 22 K, while maintaining a nearly constant $T_{\rm Av} = 1/2$ ($T_{\rm source} + T_{\rm sink}$) around 350 K

Measurement protocol was as follows: The chip containing a thermopile under test was mounted and contacted in a probe station, and the thermopile held electrically in either open circuit (OC, forced zero current) or short circuit (SC, forced zero voltage) conditions using a four-terminal source-measure unit (SMU). $T_{\rm sink}$ was set using a temperature controller operating the chuck's thermometer and heater. $T_{\rm source}$ was set by applying an appropriate $V_{\rm therm}$ bias to the thermistor using a four-terminal SMU and measuring $I_{\rm therm}$ so the resistance $R_{\rm therm}$ corresponding to a desired $T_{\rm source}$ was obtained. A slightly higher thermistor bias was always required in SC compared to OC to

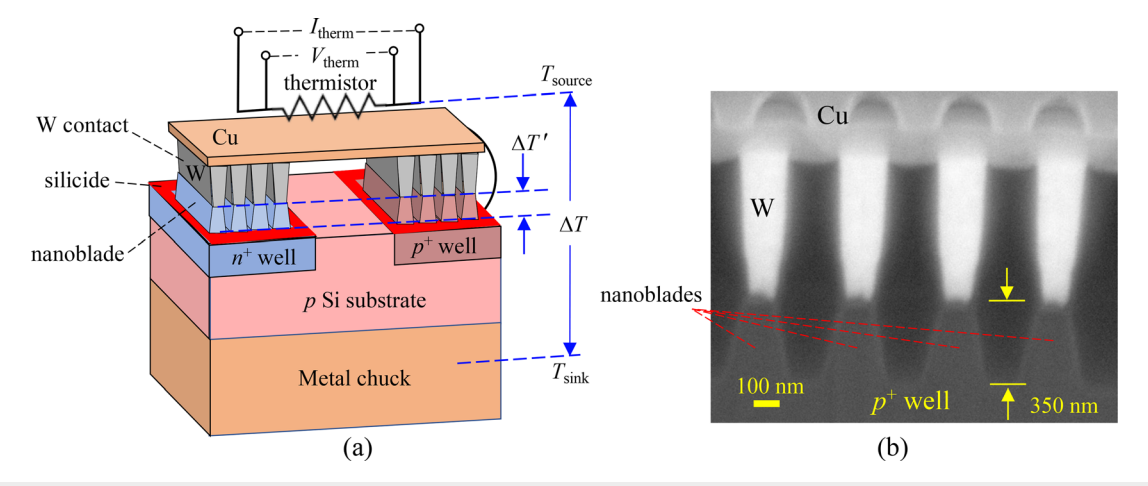


FIG. 1. (a) Schematic illustration (not to scale) of a nanoblade thermopile. n- and p-type nanoblades are grouped into arrays of four nanoblades and surrounded by silicide for electrical contact. Thermopile voltage is measured as the potential difference between the n^+ well silicide and the p^+ well silicide. (b) Cross-sectional SEM image of a four nanoblade group as circled in (a). Nanoblades are contacted from above by tungsten (W) plugs. The n- and p-sides are electrically connected in series by a copper (Cu) bridge.

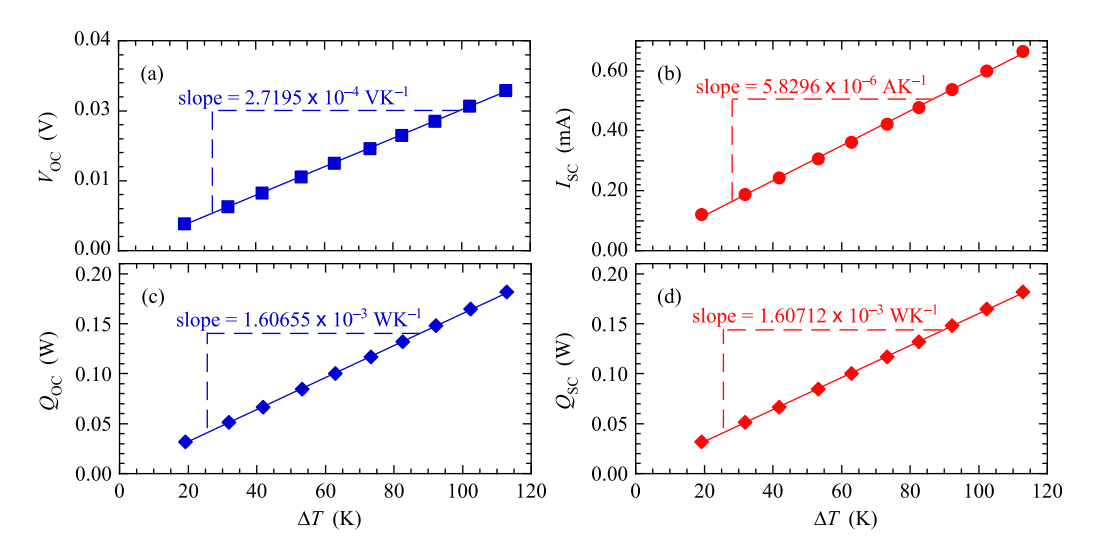


FIG. 2. Data plots of (a) open circuit voltage $V_{\rm OC}$, (b) short circuit current $I_{\rm SC}$, (c) open circuit heat flow $Q_{\rm OC}$, and (d) short circuit heat flow $Q_{\rm SC}$ all plotted against applied temperature difference ΔT . Solid lines are least-square linear fits to the data, with fitted slope values indicated.

achieve the same $R_{\rm therm}$ (hence same $T_{\rm source}$) because of the additional Peltier heat flow that occurs in SC but not OC. After setting all biases, $T_{\rm source}$ and $T_{\rm sink}$ were monitored until they stabilized to within fluctuations of ± 0.1 K, indicating the system reached steady state; this typically took 3 min. In steady state, either $V_{\rm OC}$ and $Q_{\rm OC} = V_{\rm therm}I_{\rm therm}$ (thermopile in OC) or $I_{\rm SC}$ and $Q_{\rm SC} = V_{\rm therm}I_{\rm therm}$ (thermopile in SC) were measured using 20 readings of each quantity with 1.67 s integration time. The thermopile was alternated between OC and SC twice at each $T_{\rm source}$, $T_{\rm sink}$ setting to rule out possible hysteretic effects associated with changing electrical termination.

Figure 2 shows data taken on one thermopile for (a) $V_{\rm OC}$ (b) $I_{\rm SC}$, (c) $Q_{\rm OC}$ and (d) $Q_{\rm SC}$ vs ΔT from 20 to 112 K. All measurements on this thermopile were taken with $T_{\rm Av}=356\pm2$ K. Symbols are plotted at the mean value of each dataset for each quantity at each ΔT . As determined by the standard deviations of each dataset, measurement uncertainty from instrumental noise was $\pm 6\times 10^{-6}$ V for $V_{\rm OC}$, $\pm 2\times 10^{-7}$ A for $I_{\rm SC}$, and $\pm 7\times 10^{-8}$ W for $Q_{\rm OC}$ and $Q_{\rm SC}$, so error bars would be smaller than the symbol sizes used in Fig. 2. Figure 2(a) shows $V_{\rm OC}$ is a linear function of ΔT , so $\alpha_{\rm meas}$ corresponding to this $T_{\rm Av}$ is most accurately determined from the slope of a linear fit: $\alpha_{\rm meas}(T_{\rm Av})=dV_{\rm OC}/d(\Delta T)=(2.7195\pm0.014)\times 10^{-4}$ VK $^{-1}$, where the uncertainty is the standard error of the linear regression slope coefficient.

From Ref. 30, the Peltier coefficient can be obtained as $\Pi_{\rm meas} = (Q_{\rm SC} - Q_{\rm OC})/I_{\rm SC}$, where all quantities are measured at the same $T_{\rm Av}$. Since the data plotted in Figs. 2(b)–2(d) are all linear functions of ΔT and are taken at very nearly the same $T_{\rm Av}$, to avoid inaccuracies introduced by instrumental offsets, $\Pi_{\rm meas}$ can be more accurately determined using the slopes of linear fits to the data in Figs. 2(b)–2(d), that is,

$$\Pi_{\text{meas}} = \frac{\left(\frac{dQ_{\text{SC}}}{d(\Delta T)} - \frac{dQ_{\text{OC}}}{d(\Delta T)}\right)}{\frac{dI_{\text{SC}}}{d(\Delta T)}}.$$
(1)

From the linear fits, $[dQ_{\rm SC}/d(\Delta T)-dQ_{\rm OC}/d(\Delta T)]=(5.680\pm0.068)\times10^{-7}~{\rm WK}^{-1}$, and $dI_{\rm SC}/d(\Delta T)=(5.830\pm0.054)\times10^{-6}~{\rm AK}^{-1}$. Using Eq. (1) then gives $\Pi_{\rm meas}(T_{\rm Av})=0.097\,43\pm0.002~{\rm WA}^{-1}$, where the uncertainty is determined from propagating standard errors through the calculation.

Because $(\Delta T'/\Delta T)=0.2$, parasitic thermal contact resistances cause $\alpha_{\rm meas}(T_{\rm Av})$ and $\Pi_{\rm meas}(T_{\rm Av})$ to be much lower than the true values $\alpha(T_{\rm Av})$ and $\Pi(T_{\rm Av})$ of the nanoblades. However, parasitic thermal resistances reduce $\alpha_{\rm meas}(T_{\rm Av})$ and $\Pi_{\rm meas}(T_{\rm Av})$ by the same factor, 23 so their ratio $[\Pi_{\rm meas}(T_{\rm Av})/\alpha_{\rm meas}(T_{\rm Av})]$ gives the true ratio $[\Pi(T_{\rm Av})/\alpha(T_{\rm Av})]$ of the thermopile. From this, we get $[\Pi_{\rm meas}(T_{\rm Av})/\alpha_{\rm meas}(T_{\rm Av})]=[\Pi(T_{\rm Av})/\alpha(T_{\rm Av})]=358\pm7$ K, where the uncertainty is determined by propagating the uncertainties in the numerator and denominator. The 7 K measurement uncertainty is <2% of the 358 K most probable value. For this thermopile, the relative deviation from the expected KR result of $T_{\rm Av}$ is then $[(\Pi/\alpha)/T_{\rm Av}-1]=+0.6\%$.

These measurements were repeated on four other thermopiles having identical design and made on the same wafer as the thermopile whose data are shown in Fig. 2. Table I summarizes the results. All thermopiles have an absolute deviation from the expected KR result of $|(\Pi/\alpha)/T_{\rm Av}-1|\leq 2.2\%$, with thermopile E having the largest deviation. Four of the five thermopiles show positive deviations, i.e., (Π/α) is measured to be slightly higher than $T_{\rm Av}$. This may just be a random

TABLE I. Summary of measured Kelvin relation ratios.

Thermopile label	$\Pi_{ m meas}/lpha_{ m meas}$ (K)	<i>T</i> _{Av} (K)	$\frac{[(\Pi_{\text{meas}}/\alpha_{\text{meas}})/}{T_{\text{Av}}-1]\ (\%)}$
A ^a	358 ± 7	356 ± 2	+0.6
В	353 ± 7	347 ± 2	+1.7
C	362 ± 7	357 ± 2	+1.4
D	352 ± 7	356 ± 2	-1.1
E	359 ± 7	351 ± 2	+2.2

^aData from this thermopile shown in Fig. 2 and detailed in the text.

statistical variance among five samples. It could also reflect a small systematic difference between the applied average temperature $T_{\rm Av}$ and the actual mean temperature in the thermopile nanoblades resulting from an imbalance between the thermal resistance connecting heat source to thermopile and the thermal resistance connecting thermopile heat sink.

The empirical agreement with the predicted KR result to within \sim 2% found for these TE nanostructures should be considered reasonably strong confirmation that the KR is valid for this system. Most experimental tests of the KR even on bulk TE systems show agreement to within experimental uncertainty of \sim 5% 31,32 and only rarely to better than 1%. 23,33

These nanoblades are small enough that a charge or phonon responding to thermal perturbation will on average experience at most a few, and plausibly less than one, charge-phonon or phonon-phonon energy exchanges. While the number of inelastic scattering events necessary to attain local equilibrium has never been quantitatively stated, it is unlikely that so few scattering events can yield a complete local thermodynamic equilibrium under an applied $\Delta T \neq 0$. Nonetheless, our results show no measurable deviation from the KR in these nanoblades. This suggests the KR, and by extension the ORR, may be robust beyond the strict LEA used in its derivation. We note that the electron-electron mean-free-path is estimated to be \sim 10 nm, ³⁴ so charge carriers probably establish local equilibrium among themselves in these nanoblades even if they do not thermalize with phonons. We speculate that a weaker condition of establishing local equilibrium among only charge degrees-of-freedom may be sufficient for the KR to be valid. This was indirectly suggested by Edwards et al.³⁵ whose calculations found the KR to be true in the linear response regime of a quantum dot refrigerator operating at $T \ll 1$ K where electrons never thermalize with phonons. It is of future interest to explore how small a nanostructure volume may be needed before measurable inconsistencies with the KR become apparent.

In conclusion, we have measured the ratio of the Peltier coefficient to thermopower in a set of silicon-based TE nanostructures and found that this ratio is consistent with the KR to within experimental uncertainty of 2%. This agreement holds even though the derivation of the KR uses a LEA to describe macroscopic nonequilibrium thermodynamics while these nanostructures are small enough that it is unlikely they attain a true local thermodynamic equilibrium under an applied thermal gradient. This suggests that a weaker form of the LEA requiring only local equilibrium among charge carriers, and not necessarily among other degrees-of-freedom, may be sufficient for the KR to be valid. As a practical matter, these results provide empirical evidence that the KR can continue to be used as an accurate description of the relationship between α and Π in nanostructured thermopiles down to dimensions of order an inelastic mean-free-path.

We thank Orlando Lazaro (Texas Instruments) for many useful discussions. Work at the University of Texas at Dallas was funded by the National Science Foundation Award No. DMR-2206888.

AUTHOR DECLARATIONS Conflict of Interest

The authors have no conflicts to disclose.

Author Contributions

Hari Prasad Panthi: Data curation (equal); Formal analysis (equal); Investigation (lead); Methodology (equal); Validation (lead); Writing – original draft (lead); Writing – review & editing (supporting). Ruchika Dhawan: Formal analysis (equal); Investigation (equal); Methodology (equal); Writing – review & editing (supporting). Hal Edwards: Conceptualization (equal); Formal analysis (equal); Investigation (supporting); Methodology (supporting); Resources (equal); Supervision (supporting); Writing – review & editing (supporting). Mark Lee: Conceptualization (lead); Data curation (equal); Formal analysis (equal); Funding acquisition (lead); Investigation (equal); Methodology (equal); Project administration (lead); Resources (lead); Supervision (lead); Writing – original draft (equal); Writing – review & editing (lead).

DATA AVAILABILITY

The data that support the findings of this study are available in the Harvard Dataverse repository https://doi.org/10.7910/DVN/FKSPH7 (Ref. 36).

REFERENCES

- ¹Q. Zhang, K. Deng, L. Wilkens, H. Reith, and K. Nielsch, "Micro-thermoelectric devices," Nat. Electron. 5, 333–347 (2022).
- ²A. I. Hochbaum, R. Chen, R. D. Delgado, W. Liang, E. C. Garnett, M. Najarian, A. Majumdar, and P. Yang, "Enhanced thermoelectric performance of rough silicon nanowires," Nature 451, 163–167 (2008).
- ³A. I. Boukai, Y. Bunimovich, J. Tahir-Kheli, J.-K. Yu, W. A. Goddard, and J. R. Heath, "Silicon nanowires as efficient thermoelectric materials," Nature 451, 168–171 (2008).
- ⁴H. Alam and S. Ramakrishna, "A review on the enhancement of figure of merit from bulk to nano-thermoelectric materials," Nano Energy **2**, 190–212 (2013).
- ⁵T. Ishibe, A. Tomeda, K. Watanabe, Y. Kamakura, N. Mori, N. Naruse, Y. Mera, Y. Yamashita, and Y. Nakamura, "Methodology of thermoelectric power factor enhancement by controlling nanowire interface," ACS Appl. Mater. Interfaces 10, 37709–37716 (2018).
- ⁶H.-T. Liu, Q. Sun, Y. Zhong, Q. Deng, L. Gan, F.-L. Lv, X.-L. Shi, Z.-G. Chen, and R. Ang, "High-performance in n-type PbTe-based thermoelectric materials achieved by synergistically dynamic doping and energy filtering," Nano Energy 91, 106706 (2022).
- ⁷Y. Lin, M. Wood, K. Imasato, J. J. Kuo, D. Lam, A. N. Mortazavi, T. J. Slade, S. A. Hodge, K. Xi, M. G. Kanatzidis, D. R. Clarke, M. C. Hersam, and G. J. Snyder, "Expression of interfacial Seebeck coefficient through grain boundary engineering with multi-layer graphene nanoplatelets," Energy Environ. Sci. 13, 4114 (2020).
- ⁸B. Nan, X. Song, C. Chang, K. Xiao, Y. Zhang, L. Yang, S. Horta, J. Li, K. H. Lim, M. Ibáñez, and A. Cabot, "Bottom-up synthesis of SnTe-based thermoelectric composites," ACS Appl. Mater. Interfaces 15, 23380–23389 (2023).
- ⁹In the literature this equation is variously referred to as the "1st Kelvin relation" or the "2nd Kelvin relation." Here we shall simply call it the "Kelvin relation."
- 10 L. Onsager, "Reciprocal relations in irreversible processes. I," Phys. Rev. 37, 405–426 (1931).
- ¹¹L. Onsager, "Reciprocal relations in irreversible processes. II," Phys. Rev. 38, 2265–2279 (1931).
- ¹²C. A. Domenicali, "Irreversible thermodynamics of thermoelectricity," Rev. Mod. Phys. 26, 237–275 (1954).
- ¹³Y. Demirel and V. Gerbaud, *Nonequilibrium Thermodynamics*, 4th ed. (Elsevier B.V., Cambridge, MA, 2019), Chap. 3.
- ¹⁴G. Benenti, K. Saito, and G. Casati, "Thermodynamic bounds on efficiency for systems with broken time-reversal symmetry," Phys. Rev. Lett. 106, 230602 (2011).

- ¹⁵R. Luo, G. Benenti, G. Casati, and J. Wang, "Onsager reciprocal relations with broken time-reversal symmetry," Phys. Rev. Res. 2, 022009 (2020).
- $^{16}\rm{Y}.$ Dong, "Clarification of Onsager reciprocal relations based on thermomass theory," Phys. Rev. E 86, 062101 (2012).
- ¹⁷Y.-C. Hua, T.-W. Xue, and Z.-Y. Guo, "Reversible reciprocal relation of thermoelectricity," Phys. Rev. E 103, 012107 (2021).
- ¹⁸J. M. G. Vilar and J. M. Rubi, "Thermodynamics "beyond" local equilibrium," Proc. Natl. Acad. Sci. U. S. A. 98(20), 11081–11084 (2001).
- ¹⁹D. Jou, J. Casas-Vázquez, and G. Lebon, Extended Irreversible Thermodynamics, 4th ed. (Springer, New York, 2010).
- ²⁰G. Chen, "Particularities of heat conduction in nanostructures," J. Nanopart. Res. 2, 199–204 (2000).
- ²¹N. Stojanovic, D. H. S. Maithripala, J. M. Berg, and M. Holtz, "Thermal conductivity in metallic nanostructures at high temperature: Electrons, phonons, and the Wiedemann-Franz law," Phys. Rev. B 82, 075418 (2010).
- ²²H. C. Öttinger, "On small local equilibrium systems," J. Non-Equilib. Thermodyn. 48, 149–158 (2023).
- ²³H. P. Panthi, R. Dhawan, H. Edwards, and M. Lee, "Empirical test of the Kelvin relation in a Bi₂Te₃ thermopile," Appl. Phys. Lett. 122, 122202 (2023).
- ²⁴L. Shi, D. Yao, G. Zhang, and B. Li, "Size dependent thermoelectric properties of silicon nanowires," Appl. Phys. Lett. 95, 063102 (2009).
- ²⁵J. H. Oh, M. Shin, and M. G. Jang, "Phonon thermal conductivity in silicon nanowires: The effects of surface roughness at low temperatures," J. Appl. Phys. 111, 044304 (2012).
- ²⁶G. Hu, H. Edwards, and M. Lee, "Silicon integrated circuit thermoelectric generators with a high specific power generation capacity," Nat. Electron. 2, 300–306 (2019).

- ²⁷R. Dhawan, P. Madusanka, G. Hu, J. Debord, T. Tran, K. Maggio, H. Edwards, and M. Lee, "Si_{0.97}Ge_{0.03} microelectronic thermoelectric generators with high power and voltage densities," Nat. Commun. 11, 4362 (2020).
 ²⁸Y. Ohishi, J. Xie, Y. Miyazaki, Y. Aikebaier, H. Muta, K. Kuorsaki, S. Yamanaka,
- ²⁸Y. Ohishi, J. Xie, Y. Miyazaki, Y. Aikebaier, H. Muta, K. Kuorsaki, S. Yamanaka, N. Uchida, and T. Tada, "Thermoelectric properties of heavily boron- and phosphorus-doped silicon," Jpn. J. Appl. Phys., Part 1 54, 071301 (2015).
- ²⁹R. Dhawan, P. Madusanka, G. Hu, K. Maggio, H. Edwards, and M. Lee, "Maximizing performance of microelectronic thermoelectric generators with parasitic thermal and electrical resistances," IEEE Trans. Electron Devices 68, 2434–2439 (2021).
- ³⁰R. Dhawan, H. P. Panthi, O. Lazaro, A. Blanco, H. Edwards, and M. Lee, "Independent determination of Peltier coefficient in thermoelectric devices," Appl. Phys. Lett. 120, 183901 (2022).
- ³¹D. G. Miller, "Thermodynamics of irreversible processes: The experimental verification of the Onsager reciprocal relations," Chem. Rev. 60, 15–37 (1960).
- ³²A. D. Avery and B. L. Zink, "Peltier cooling and Onsager reciprocity in ferromagnetic thin films," Phys. Rev. Lett. 111, 126602 (2013).
- 33J. Jimenez, E. Rojas, and M. Zamora, "Device for simultaneous measurement of the Peltier and Seebeck coefficients: Verification of the Kelvin relation," J. Appl. Phys. 56, 3250–3255 (1984).
- ³⁴B. Qiu, Z. Tian, A. Vallabhaneni, B. Liao, J. M. Mendoza, O. D. Restrepo, X. Ruan, and G. Chen, "First-principles simulation of electron mean-free-path spectra and thermoelectric properties in silicon," Europhys. Lett. 109, 57006 (2015).
- 35H. L. Edwards, Q. Niu, G. A. Georgakis, and A. L. de Lozanne, "Cryogenic cooling using tunneling structures with sharp energy features," Phys. Rev. B 52, 5714–5736 (1995).
- ³⁶M. Lee, data for "Empirical Test of the Kelvin Relation in Thermoelectric Nanostructures," Harvard Dataverse, https://doi.org/10.7910/DVN/FKSPH7